In Situ Study on Kinetic Behavior during Asymmetric Membrane Formation via Phase Inversion Process Using Raman Spectroscopy

H. J. KIM, A. E. FOUDA, K. JONASSON

Institute for Chemical Process and Environmental Technology, National Research Council Canada, Ottawa, Ontario K1A 0R6, Canada

Received 2 February 1999; accepted 29 May 1999

ABSTRACT: Asymmetric membrane formation has been studied by using an *in situ* analysis developed with a Micro Raman spectroscopy, which emphasizes kinetic aspects of the phase inversion process. Changes in composition with time was successfully measured on the gelation bath-side as well as inside the precipitated phase for the polymer/solvent/nonsolvent system of polysulfone/1-methyl-2-pyrrolidinone/ethanol. The results shows that resulting relative mass transfer rates of solvent and nonsolvent during the phase inversion process strongly influence the final membrane morphologies. In addition, ternary compositions at which phase separation initiates were explored by analyzing the coagulation front. © 2000 John Wiley & Sons, Inc. J Appl Polym Sci 75: 135–141, 2000

Key words: asymmetric membranes; phase inversion process; micro Raman spectroscopy

INTRODUCTION

Asymmetric microporous polymer membranes are widely prepared by the phase inversion process during which a thin layer of a viscous polymer solution is spread and then immersed in a gelation medium of nonsolvent. Complicated phenomena are involved in this process, such as phase separation of a homogeneous polymer solution into two phases, polymer-rich and polymer-lean, and diffusive interchange between the solvent and nonsolvent. The former is regarded as a thermodynamic effect, while the latter is a kinetic one. There have been many studies analyzing this process in terms of thermodynamic and kinetic aspects.[1–4] Thermodynamic studies were mainly focused on the relationships between casting conditions and final morphologies of the membranes, whereas kinetic studies have related the mass transfer rates of polymer solution and gelation medium occurring at the interface to pore size distribution, skin, and macrovoid formation.[5–7] It has been demonstrated that the relative exchange rate of solvent and nonsolvent across the interface leads to a range of resulting asymmetric membrane morphologies.

Kinetic measurements have been carried out mainly using optical set-ups[8] or monitoring a refractive index gradient profile bath-side of the interface.[9–11] Because of the limitations of those methods, only a qualitative growth of precipitated phase can be observed or only the solvent concentration in the gelation bath can be detected. In this study, a Micro Raman spectroscopy technique was developed to monitor the composition change in the precipitated phase as well as in the bath. As a molecular characterization tool, Ra-

Correspondence to: H. J. Kim.
NRCC No. 41997.

Journal of Applied Polymer Science, Vol. 75, 135–141 (2000)
 CCC 0021-8995/00/010135-07

man spectroscopy is used to identify bonding and functional groups. Interactions between molecular units and their surroundings also can be readily detected by perturbations in the Raman spectrum. Hydrogen bonding, crystal field splitting, chain conformation, chain packing, and solvation are all examples of modifications to the surrounding electrical field of the molecular unit that will affect the Raman scattering. Chain conformation and packing changes have been studied in the melting of poly(1-methyladenylic acid)[12] and solvent effects on the sol-gel polymerization used to form silica sols.[13] Polyacrylamide gels with varying cross-link concentration have been investigated.[14] Chain environments of polymers, effects of ion clustering, or pairing on the Raman spectrum are demonstrated.[15] A recently reported technique, Micro Raman[16] provides the advantages of increased spatial resolution by sampling areas on the order of a square micrometer, low laser powers due to the concentration of light by the microscope, imaging of the sample and area discrimination, smaller samples needed, and minimization of fluorescence from some sources. Most evident examples are studies on single crystal lamellae, polymer interfaces, phase separations, oriented material, composite systems, and thin films.[16–19] Similarly, spatial resolution has been used to study the transport of solvents in polymers.[20] In this paper, the kinetic phenomena during asymmetric membrane formation will be studied using Micro Raman spectroscopy emphasizing spatially and time resolved composition change in the vicinity of the interface between the polymer solution and the gelation medium as well as in the coagulation front.

EXPERIMENT

Materials

Polysulfone (PSF, Udel 3500, MW = 50,000) was the polymer used in this study. Reagent grade 1-methyl-2-pyrrolidinone (NMP, Aldrich) was used as received for the solvent and absolute ethanol (EtOH, Aldrich) was used as nonsolvent. Polymer solutions were filtered through PTFE membranes (Cole-Parmer Instrument Co.) with 0.5-μm pore size.

Optical Microscope and SEM Analysis

Phase separation of the polymer solution was observed by optical microscope at magnifications of 25 and 90, during precipitation in ethanol. Details of the experimental method were described elsewhere.[21] The cross-sectional membrane morphology was examined by a scanning electron microscopy (SEM, Jeol ISM 5300).

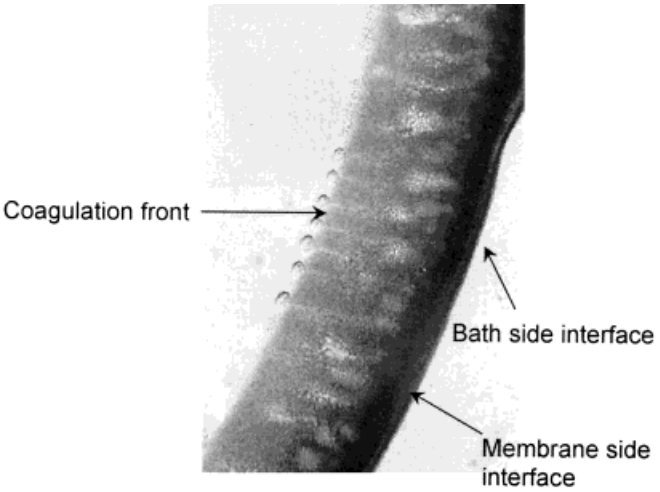

Figure 1 Microscopic picture of phase inversion process. Spectra were taken at three different spots as a function of time.

Micro Raman Experiment

Raman spectra were excited with a He/Ne laser (Dilor), operated at a power level of 25 mW and a frequency of 632.8 nm. The polymer solution was held between two optical grade slide glass with a 130-μm space between them. The laser beam is focused to a 10-μm sample point, which is positioned at the different sites of interest. All the measurements were performed at room temperature. Figure 1 illustrates the various interest sites that were studied during membrane formation in this study.

RESULTS AND DISCUSSION

It is well known that membrane morphology strongly depends on the composition of the precursor polymer solution as shown in Figure 2. As the polymer concentration increases, the final morphology of the membrane becomes more sponge-like and macrovoid-free. Figure 3 shows a Raman spectrum of polysulfone. The Raman modes of the polysulfone sample were assigned with reference to several cited references.[22,23] The assignments are summarized as follows: the band

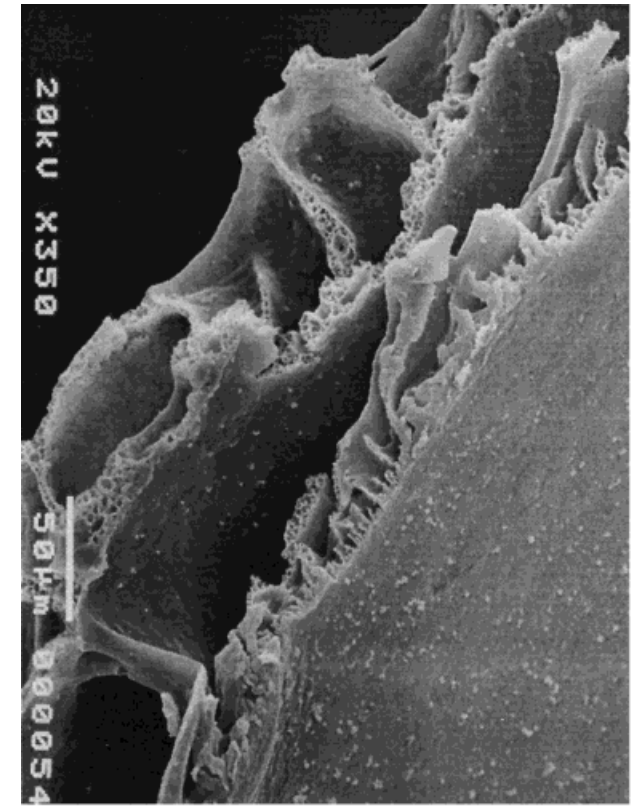

(a)

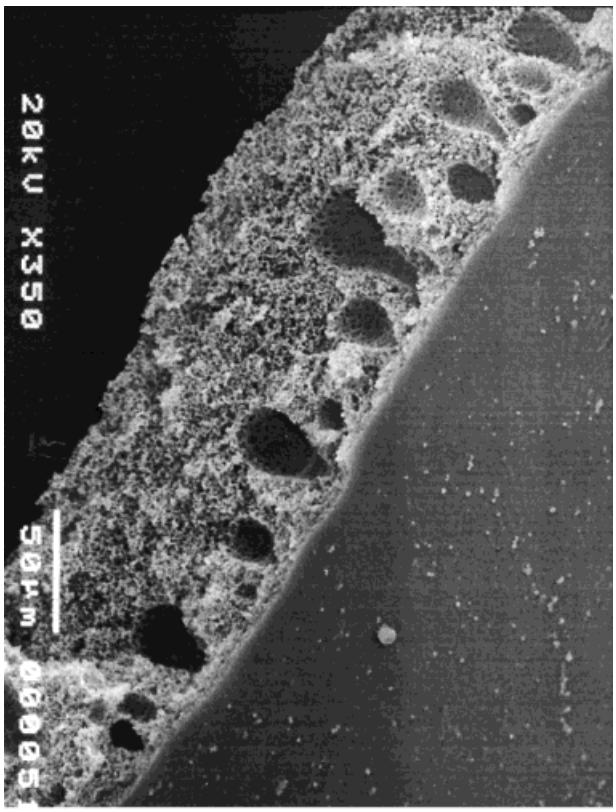

(b)

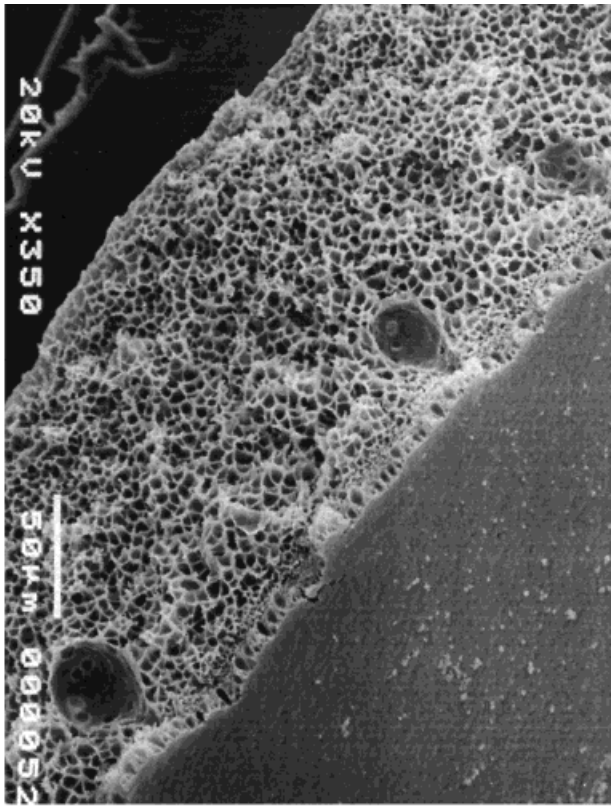

(c)

at 739.3 cm^{-1} is the result of antisymmetric C—S—C stretching and shows an intense band due to out-of-plane benzene ring C—H deformation at 788.1 cm^{-1}, which will be used in this study to measure the polysulfone concentration in ternary system during precipitation; two bands at 1073.3 and 1108.3 cm^{-1} are attributed to symmetric and antisymmetric SO_2 stretching, respectively, where the symmetric C—O—C stretching mode is strongly recognized at 1149.5 cm^{-1} and weak the antisymmetric mode occurs at 1203.9 cm^{-1}; the band at 1585.6 and 1606.6 cm^{-1} corresponds to a phenyl ring vibration, and at 3070.8 cm^{-1} a C—H stretching mode is observed. Raman spectra of EtOH and NMP are illustrated in Figure 4. Detailed peak assignment can be found in several references.[24,25] The area of bands at 877.8 cm^{-1} for EtOH (symmetric C—C—O stretching) and 924.8 cm^{-1} for NMP (C—C stretching) were chosen for quantitative analysis for each sub-

Figure 2 SEM pictures of membranes prepared from different polymer concentrations: (a) 10 wt %, (b) 20 wt %, and (c) 30 wt % of polysulfone in NMP, respectively.

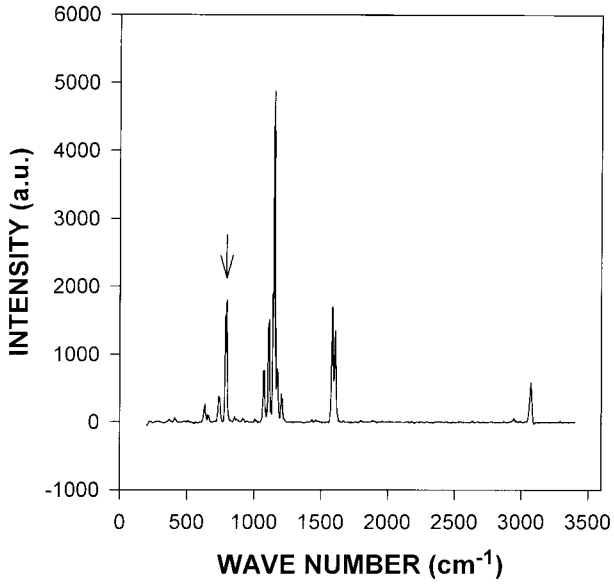

Figure 3 Raman spectrum for polysulfone.

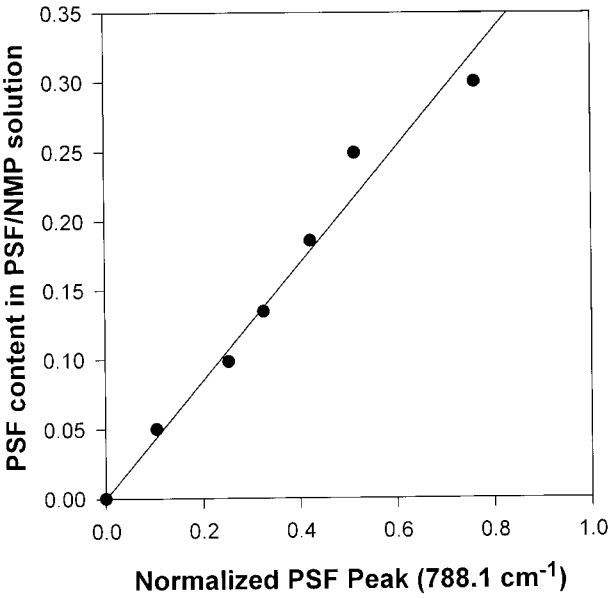

Figure 5 Calibration curve for polysulfone in NMP.

stance, respectively. Calibration results for PSF/NMP and NMP/EtOH are shown in Figures 5 and 6. The measured spectra were converted to specific concentration based on the calibration results. Raman spectra measured on the bathside of the polymer solution-nonsolvent interface were recorded as a function of time for 20 wt % polymer solution, the results of which are shown in Figure 7. The NMP concentration decreases as time elapses, which is thought to be the result of membrane skin developing during the precipitation. Other spectra were taken at 2.5 minutes after precipitation for different concentration polymer solutions (Fig. 8). For a higher polymer concentration solution, it is observed that a relatively lower amount of NMP is detected. This can be explained that with a higher polymer concentration, the skin is formed thicker and faster, preventing solvent molecules from diffusing out to bathside. The change of NMP concentration at

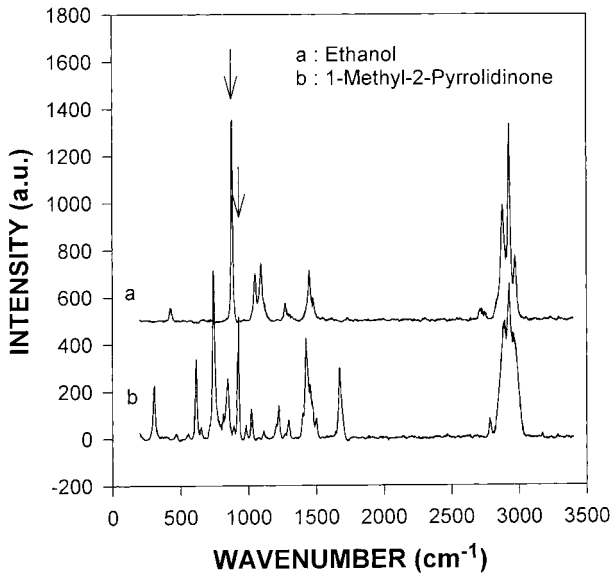

Figure 4 Raman spectra for NMP and ethanol.

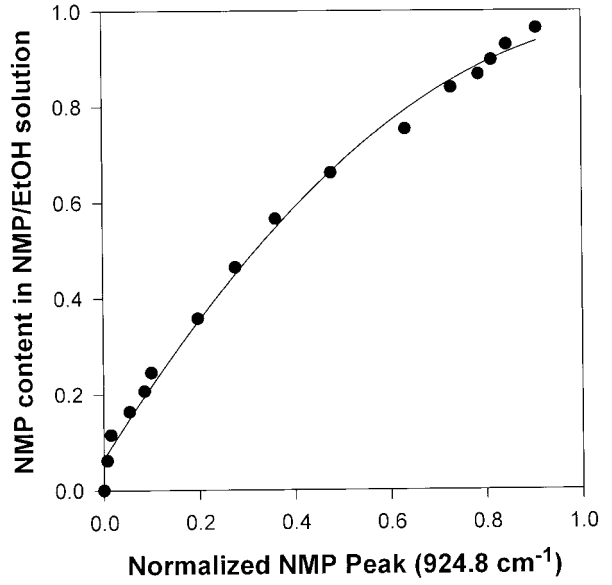

Figure 6 Calibration curve for NMP in ethanol.

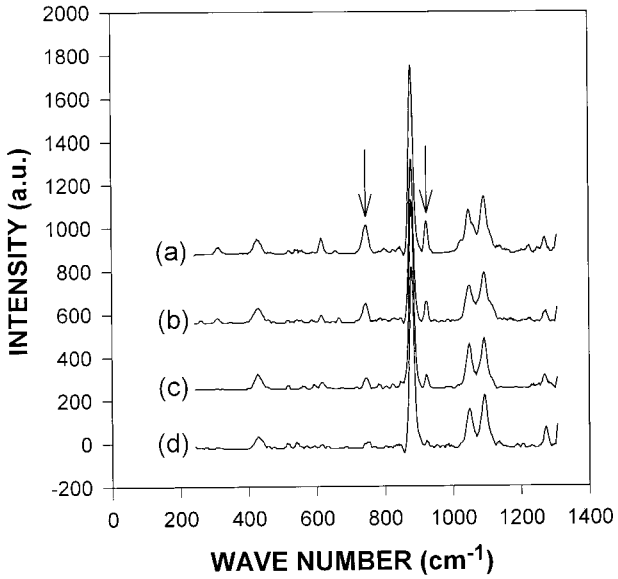

Figure 7 Raman spectra in bathside interface as a function of time for 20 wt % polymer solution: (a) 0.5, (b) 2.0, (c) 4.0, and (d) 7.0 min after precipitation.

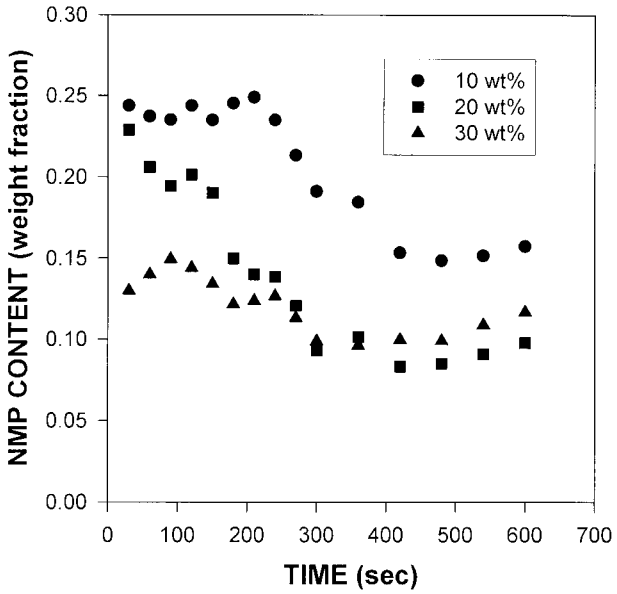

Figure 9 Change of NMP concentration at bath-side interface as a function of time.

bathside interface is plotted against time and polymer concentration in Figure 9. It decreases for all cases until about 5 min after precipitation. We believe that the NMP concentration at bathside interface increases too fast to be spectroscopically detected at the initial moment of the precipitation. During this initial period, membrane skin is formed and then starts preventing mass exchange of solvent and nonsolvent. This causes the solvent concentration at bathside interface to decrease because the rate of solvent diffusing out from the precipitated phase into the bathside interface decreases until it reaches to equilibrium that the rate of solvent coming into the bathside interface becomes the same as that diffusing into bulk coagulation bath. Then it shows no change in solvent concentration as a function of time. The phase separation for asymmetric membrane formation is kinetically completed during this period. The higher the polymer concentration of the solution is, the denser and thicker the developing membrane skin, resulting in lower solvent concentration at bathside interface. Raman spectra on membrane side interface were recorded and are shown in Figure 10. Polymer concentration (788 cm^{-1}) increases, whereas EtOH concentration decreases with time. The NMP concentration hardly changes. As explained above, dense skin is readily formed in the early stage of precipitation as a result of very fast mass exchange between solvent and nonsolvent. In this period, the nonsolvent concentration increases so fast that it can hardly be detected spectroscopically as a function of time; then the skin starts to hinder the mass exchange, preventing more nonsolvent from diffusing in, while the nonsolvent molecules that already came in diffuse down to the bulk polymer

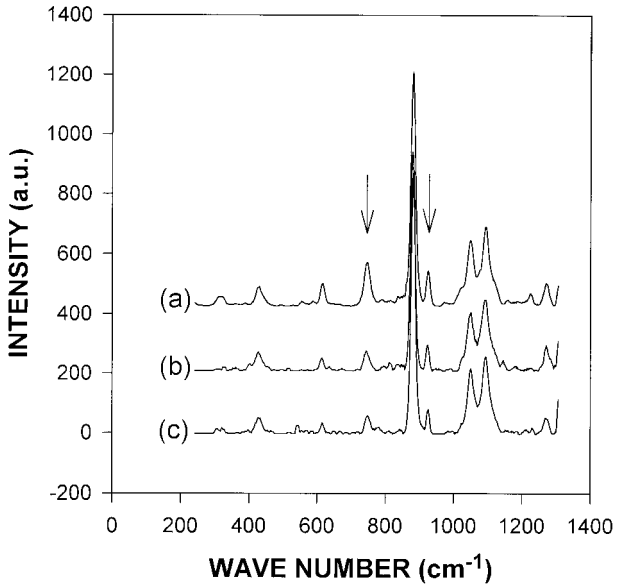

Figure 8 Raman spectra in bathside interface as a function of polymer concentration at 2.5 min after precipitation: (a) 10 wt %, (b) 20 wt %, and (c) 30 wt % of polysulfone in NMP, respectively.

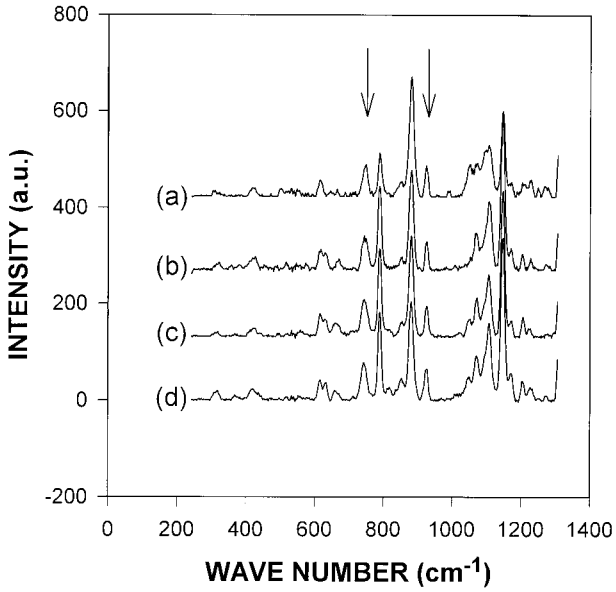

Figure 10 Raman spectra in membrane side interface as a function of time for 20 wt % polymer solution: (a) 0.5, (b) 2.5, (c) 3.5, and (d) 5.0 min after precipitation.

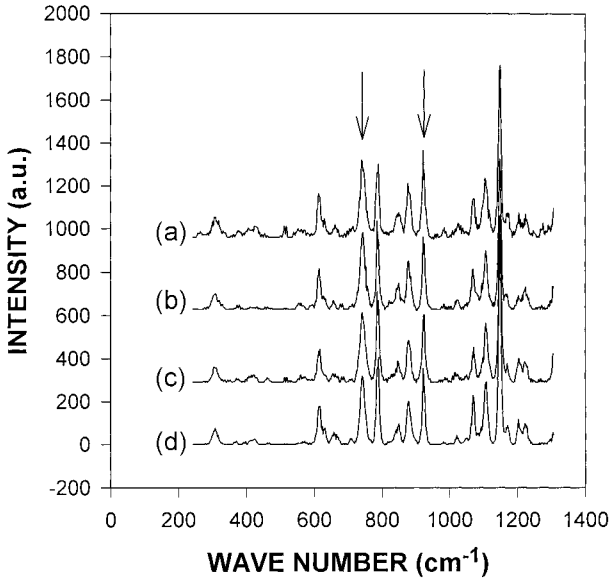

Figure 11 Raman spectra at coagulation front as a function of time for 20 wt % polymer solution: (a) 1.0, (b) 2.0, (c) 5.0, and (d) 7.0 min after precipitation.

solution. Meanwhile, the solvent concentration does not change very much because it is still easier for solvent molecules to diffuse up to the membrane side interface from the bulk polymer solution. On the other hand, the polymer concentration increases, because polymer chains aggregate, forming the polymer-rich phase, which is a much slower process than mass exchange between solvent and nonsolvent, so that it can be kinetically monitored with spectroscopic method. By the results of Figures 7 through 10 compared to Figure 2, it can be concluded that the mass transfer rate of solvent and nonsolvent strongly affects the membrane morphology. Figures 11 and 12 show the composition change at the coagulation front as a function of time and polymer concentration. It does not change much with time but varies quite a bit with polymer concentration. This means the ternary system phase separates in the thermodynamic equilibrium state. In other words, it is independent of time but strongly depends on thermodynamic parameters, such as solution composition or temperature, whereas the situation at the bathside interface or membrane interface is kinetic. Averaged compositions of repeated measurements are summarized in Table I. The figures can be considered as exact compositions for these polymer solutions to start phase separation, which corresponds to the cloud points in the ternary diagram.

CONCLUSIONS

The result of this study indicates that the *in situ* experiment on kinetic behavior in asym-

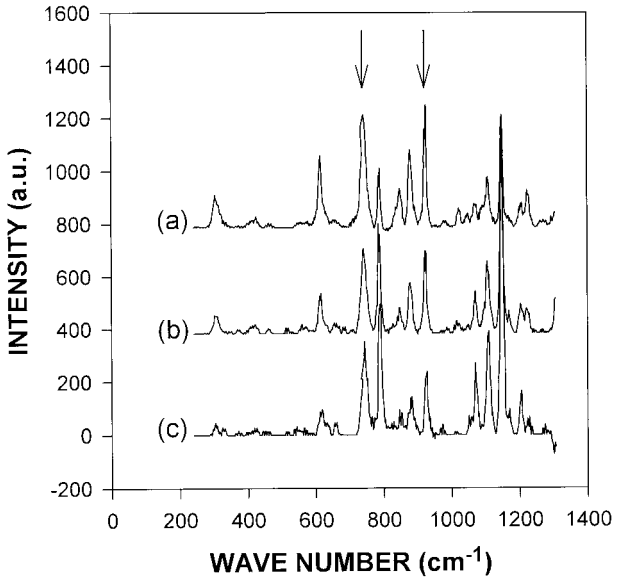

Figure 12 Raman spectra at coagulation front at 5 min after precipitation for different polymer concentration solutions: (a) 10 wt %, (b) 20 wt %, and (c) 30 wt % of polysulfone in NMP, respectively.

Table I Composition Change at Coagulation Front

Polymer Concentration in Dope Solution (wt %)	PSF	NMP	EtOH
10	0.090	0.258	0.653
20	0.174	0.218	0.609
30	0.235	0.179	0.587

Values are weight fraction.

metric membrane formation was successfully carried out with Micro Raman spectroscopy. The concentration change was easily measured quantitatively at any spot during membrane formation. From the spectroscopic result, the qualitative kinetic comparison between polymer solutions during phase inversion process in asymmetric membrane formation can be related to the final membrane morphology. Additionally, thermodynamic study to verify the ternary composition at which phase separation takes place was carried out by the coagulation front analysis experiment.

REFERENCES

1. Strathmann, H.; Kock, K. Desalination 1977, 21, 241.
2. Cohen, C.; Tanny, G. B.; Prager, S. J Polym Sci Polym Phys Ed 1979, 17, 477.
3. Wijmanns, J. G.; Kant, J.; Mulder, M. H. V.; Smolders, C. A. Polymer 1985, 26, 1539.
4. Reuvers, A. J.; Altena, F. W.; Smolders, C. A. J Polym Sci Polym Phys Ed 1986, 24, 793.
5. Strathmann, H. In Material Science of Synthetic Membranes; Lloyd, D. R., Ed.; ACS Symposium Series 269; American Chemical Society: Washington, DC, 1985.
6. Reuvers, A. J.; van den Berg, J. W. A.; Smolders, C. A. J Membr Sci 1987, 34, 45.
7. Reuvers, A. J.; Smolders, C. A. J Membr Sci 1987, 34, 67.
8. Cabasso, I. In Synthetic Membranes: Desalination; Turbak, A. F., Ed.; ACS Symposium Series 153, American Chemical Society, Washington, DC, 1981, p. 267.
9. Yilmaz, L.; McHugh, A. J. J Membr Sci 1988, 28, 287.
10. Gaides, G. E.; McHugh, A. J. J Membr Sci 1992, 74, 83.
11. van de Witte, P.; van den Berg, J. W. A.; Feijen, J.; McHugh, A. J. J Appl Polym Sci 1986, 61, 685.
12. Klamp, H.; Strum, J.; Peticolas, W. L. Ber Bunsenges Phys Chem 1981, 85, 661.
13. Artaki, I.; Zerda, T. W.; Jonas, J. J Non-Cryst Solids 1986, 81, 381.
14. Bansil, R.; Gupta, M. K. Ferroelectrics 1980, 30, 63.
15. Neppel, A.; Butler, I. S.; Brockman, N.; Eisenberg, A. J Macromol Sci Phys 1981, B19, 61.
16. Anderson, M. E.; Muggli, R. Z. Anal Chem 1981, 53, 1772.
17. Tanaka, H.; Ikeda, T.; Nishi, T. Appl Phys Lett 1986, 48, 393.
18. Adar, F.; Noether, H. Polymer 1985, 26, 1935.
19. Cook, C. J. Laser Microprobe Analysis and Laser Raman Spectroscopy Analysis Techniques for Identification of Organic surface Contaminates, Abstr. 25335, Energy Res Abstr 1987.
20. Klier, J.; Peppas, N. A. Polym Bull 1986, 16, 359.
21. Kang, Y. S.; Kim, H. J.; Kim, U. Y. J Membr Sci 1991, 60, 219.
22. Adams, W. F. Spectrochim Acta 1994, 50A, 1967.
23. Stuart, B. H. Spectrochim Acta 1997, 53A, 107.
24. Tanaka, N.; Ito, K.; Kitano, H.; Ise, N. Spectrochim Acta 1992, 48A, 237.
25. Dollish, F. R.; Fateley, W. G.; Bentley, F. F. Characteristic Raman Frequencies of Organic Compounds; John Wiley & Sons: New York, 1974.